Curr Radiol Rep (2019) 7:25
https://doi.org/10.1007/s40134-019-0338-4

Imaging of Emerging Infectious Diseases

Meghan Jardon[1,3] · Shaden F. Mohammad[2] · Cecilia M. Jude[2] · Anokh Pahwa[2]

Published online: 11 July 2019

Abstract
Purpose of Review Emerging infectious diseases have seen a record increase in prevalence, and understanding their management is critical in an increasingly global community. In this paper, we review current literature detailing the role of radiology in the diagnosis and treatment of the Ebola (EVD), Zika (ZVD), Chikungunya (CHIKF), H1N1, Middle East Respiratory (MERS), and Severe Acute Respiratory Syndrome (SARS) viruses.
Recent Findings Complex protocols are required to safely use portable imaging in EVD to prevent nosocomial spread of disease. In ZVD, antenatal ultrasound can detect fetal abnormalities early, allowing implementation of care and support to affected families. Imaging is useful in assessing the extent of involvement of chronic CHIKF and monitoring treatment effect. Chest radiography and CT play a more direct role in the diagnosis and monitoring of the viral infections with primarily respiratory manifestations (H1N1, MERS, and SARS).
Summary Radiology plays a variable role in emerging infectious diseases, requiring an understanding of disease transmission and safe imaging practices, as well as imaging features that affect clinical management.

This article is part of the Topical collection on *Global Radiology*.

✉ Meghan Jardon
mjardon@mednet.ucla.edu

[1] Department of Radiological Sciences, University of California Los Angeles, Los Angeles, CA, USA

[2] Department of Radiological Sciences, Olive View - UCLA Medical Center, Sylmar, CA, USA

[3] Department of Radiological Sciences, Ronald Reagan UCLA Medical Center, University of California Los Angeles, 757 Westwood Plaza, Suite 1638, Los Angeles, CA 90095, USA

Keywords Emerging disease · Ebola · Zika · Chikungunya · H1N1 · MERS · SARS

Introduction

Emerging infectious diseases, defined by the Centers for Disease Control and Prevention (CDC) as those whose "incidence in humans has increased in the past two decades or threaten[s] to increase in the near future," have seen a record increase in prevalence over the past two decades related to increased international travel, developing antibiotic resistance, and increased industrialization and globalization of food production and distribution [1, 2]. Emerging infectious diseases are now recognized at an alarming rate of one per year, resulting from emergence of novel infectious agents or re-emergence of previously described diseases [1]. In this paper, we explore the utility of various imaging techniques in the evaluation and management of emerging infectious diseases. These include diseases with systemic manifestations caused by the Ebola, Zika, and Chikungunya viruses, and infections with predominantly respiratory manifestations caused by H1N1, MERS, and SARS viruses. While Multi- and Extensively Drug Resistant Tuberculosis continue to play an important role as emerging infectious diseases, this topic is beyond the scope of this work. An approach to imaging in resource-limited settings will also be discussed, with an emphasis on the necessary safety precautions to prevent nosocomial spread of these infectious agents.

Ebola Virus Disease (EVD)

The Ebola viruses are a group of RNA viruses in the Filoviridae family, initially isolated in humans in the Democratic Republic of Congo (formerly Zaire) in 1976 [3]. Small outbreaks have occurred in Africa since its discovery, with population growth and direct interaction with wildlife contributing to increased spread of the virus. There are four viral strains in the genus Ebolavirus that cause disease in humans, with an overall average fatality rate of 50% [4]. The more virulent Zaire Ebolavirus has a 67% fatality rate and was responsible for the West African Epidemic of 2013 that started in Guinea and quickly spread to Liberia and Sierra Leone. The epidemic peaked in 2014 and ended in 2016, and was the largest recorded EVD outbreak with over 28,000 cases and 11,000 deaths (although the magnitude of the outbreak is likely underestimated) [3]. EVD is ongoing, with recent smaller outbreaks in the Democratic Republic of Congo in 2018 [5]. African fruit bats are believed to be the reservoir host for humans and other primates.

The Ebola virus is spread through the bodily fluids of infected persons, and enters its new hosts via mucous membranes or broken skin [6]. The incubation period lasts 3–21 days, followed by symptoms of fever, severe headache, myalgia, malaise, diarrhea and vomiting, and, in severe cases, hemorrhage [7]. A key component of EVD management is containment and control of the highly contagious infection, including contact tracing, use of personal protective equipment, and safe burial practices. Treatment is supportive, including intravenous fluid and electrolyte repletion. Additional supportive methods such as mechanical ventilation and temporary hemodialysis are sometimes utilized in the developed world, but are unavailable in resource-limited settings, where treatment is often limited to oral rehydration [8••]. A recombinant Zaire Ebola vaccine, with high efficacy for the Zaire strain, was first used in 2018 to stop an outbreak in the Democratic Republic of Congo.

The role of radiology in the evaluation and management of patients with EVD is limited [8••, 9]]. Due to its systemic, non-specific manifestations, imaging is most useful for monitoring supportive treatment, rather than evaluating the direct effect of the disease on specific organs [7, 8••]. Although infrequently available in resource-limited settings, when supportive measures like central venous access or mechanical ventilation are accessible, more specific indications for imaging exist. For example, point of care ultrasound (US) is useful for central venous catheter placement and assessing for associated complications, such as pneumothorax or deep venous thrombosis [10]. Chest radiography is useful in monitoring cardiopulmonary status, assessing central line and endotracheal tube placement, and determining when aggressive measures like endotracheal intubation are indicated [10].

When imaging of patients with EVD is indicated and adequate resources are available, implementing safe and effective procedures presents a unique challenge. Additional supplies and personnel are required due to increased protective measures needed to safely acquire images [9]. Ebola virus is transferred via infected bodily fluids, which can survive on surfaces for days to weeks. Medical imaging equipment must be decontaminated before use on other patients, limiting imaging modalities to portable techniques (radiographs and US) [6, 8••]. The utilization of CT and MRI would increase the risk of transmission to patients and healthcare workers [11] and is often unavailable in regions affected by EVD.

In 2015, Emory University published their protocols for safely obtaining portable US and chest radiographs in their Ebola isolation unit, which includes a multi-step process involving multiple staff members, multiple plastic coverings over imaging equipment, and utilization of an anteroom to prepare and sanitize equipment entering or leaving the patient's room [8••, 12]. Other hospitals have developed similar protocols and successfully prevented the spread of Ebola virus to healthcare workers treating their Ebola patients [7, 9]. When developing a protocol for safely imaging patients with Ebola virus, it is important to use products that adequately kill the virus without damaging the medical equipment. For example, chlorine-based cleaning products may cause erosion of the electrical contact plates of US batteries and charging docks [10]. Ideally, a fully digital system where the x-ray detector can transmit images wirelessly should be used. This would allow the equipment to remain in the patient's room throughout treatment. However, this is usually not available in areas affected by EVD [7, 8••].

The World Health Organization (WHO) estimates that 3–4% of patients infected with Ebola are healthcare workers, which highlights the importance of prevention of nosocomial spread [13]. Minimizing the number of hospital staff that come in contact with patients or infected bodily fluids is an important step. Although ultrasounds and radiographs are typically acquired by technologists, other members of the treatment team can be trained to acquire images, in order to decrease the risk of exposure [8••].

The role of imaging patients with EVD in resource-limited settings is therefore reserved for specific indications, utilizing portable US and portable chest radiography. Imaging of patients with this highly contagious infection must adhere to strict protocols that provide the necessary diagnostic information while preventing disease transmission.

Zika Virus Disease (ZVD)

The Zika virus is an arbovirus in the family Flaviviridae that was initially isolated in 1947 in a macaque monkey in the Zika forest in Uganda, and in 1952 in humans. Initially confined to an equatorial belt from Africa to Southeast Asia, the infection spread eastward to the Americas between 2007 and 2016 [14]. Two small outbreaks in Micronesia in 2007 and in Oceania in 2013–2014 preceded the largest epidemic of ZVD in 2015, which started in Brazil and quickly spread throughout North, Central and South America, and the Caribbean [14]. Anthropogenic climate change with warmer temperature and increased precipitation facilitated the epidemic spread, which lasted from 2015 through 2016. ZVD affected an estimated 1.5 million people in Brazil, resulting in over 3800 cases of microcephaly [14]. The primary route of Zika virus transmission is through the bite of an infected Aedes aegypti or Aedes albopictus mosquito [14]. Once infected, human-to-human transmission occurs through either vertical transmission (from an infected pregnant woman to the fetus) or sexual transmission [15]. The majority of infections are asymptomatic.

If clinically apparent, the presentation of ZVD is usually mild and non-specific, including fever, maculopapular rash, conjunctivitis, arthralgias, and fatigue that last up to 1 week [14]. In fetuses and neonates, infection with Zika virus may cause congenital Zika syndrome. Congenital infection causes direct cellular injury to brain tissue, resulting in microcephaly and retinal damage, with less common defects including congenital contractures and hypertonia. In adults and older children, Zika infection may cause several neurologic manifestations, including Guillain–Barre Syndrome and neuropathy [16]. The WHO recommends continued vigilance for Zika virus infection, which continues to spread due to climate change, urbanization, and globalization [17]. There is no specific treatment for Zika infection, although several vaccines entered clinical trials in 2017.

Zika virus conveys a disproportionate risk to low-resource areas, as many of the countries it affects lack the medical facilities to run diagnostic tests [14]. There is significant overlap in symptomatology between Zika, Chikungunya, and Dengue infections, and without proper laboratory diagnosis, distinguishing between these endemic viral illnesses is challenging. The primary role of radiology in ZVD is prenatal screening in those suspected of having congenital infection. Prenatal ultrasound allows for early detection of Zika-associated fetal abnormalities and facilitates early implementation of care and support to affected families, one of the objectives outlined in the WHO Zika Strategic Response Plan [17].

US is particularly suitable for antenatal screening in resource-limited settings, as it is a safe, inexpensive, and accessible method of evaluation. In suspected congenital Zika syndrome, the CDC recommends US be considered every 3–4 weeks to monitor fetal growth and assess for signs of infection and anomalous fetal development [15]. The most common prenatal ultrasound finding is microcephaly, defined as head circumference more than two standard deviations below the mean for gestational age [18•]. However, prenatal normocephaly does not exclude congenital Zika infection, as microcephaly can develop after birth. A study of expectant mothers with confirmed Zika infection in Colombia found a 15- to 24-week delay between maternal diagnosis and development of fetal microcephaly, with the earliest detection at 24-week gestational age [15]. Therefore, detailed fetal neuroimaging throughout pregnancy is warranted in cases of suspected or confirmed infection, as a normal fetal US before 24-week gestation age does not exclude the possibility of developing congenital Zika syndrome.

Additional intracranial US findings include cerebral parenchymal atrophy and associated ventriculomegaly, subependymal pseudocysts, ocular abnormalities, and hypoplasia or agenesis of the corpus callosum, cerebellum, and brainstem [18•]. Parenchymal calcifications can also occur, and are typically located at the gray–white matter junction. Non-neurologic US findings are less specific and include echogenic bowel, hepatosplenomegaly with hepatic calcifications, and talipes equinovarus [15, 19].

Magnetic Resonance Imaging (MRI) provides a more detailed assessment of the neurologic manifestations of congenital Zika syndrome, either prenatally or postnatally. However, MRI is often not available in resource-limited settings [20]. MRI findings are similar to US, although MRI provides a clearer delineation of patterns of cortical atrophy, white matter abnormalities related to abnormal myelination, and hypoplasia of the corpus callosum, cerebellum, and brainstem (Fig. 1) [18•, 21].

Postnatal Computed Tomography (CT) can also assess for congenital anomalies, although it is not as easily accessible as US. CT is a sensitive method for detecting parenchymal calcifications and, unlike US, does not require open fontanelles for imaging. The lower cost of CT and increased availability compared to MRI make it more feasible in resource-limited areas. CT findings of congenital Zika include dystrophic parenchymal calcifications with typical distribution at or below the corticomedullary junction, which decrease in size and number over time [20]. Other findings include secondary effects of global cerebral cortical volume loss, such as ventriculomegaly, discrepancy between cranium and facial size, cranial bone collapse with protuberance of the occipital bone, and small fontanelles [18•, 20]. CT is also useful in monitoring for

Fig. 1 Infant with confirmed congenital Zika virus infection, with diffuse cortical atrophy and hypoplasia of the corpus callosum, cerebellum, and brainstem. **a** Coronal fluid-attenuated T2, **b** sagittal fluid-attenuated T2, **c** axial fat-saturated T1 and **d** sagittal T2 weighted MRI demonstrate these findings Images courtesy of Drs. Nielsen and Adachi, UCLA Department of Pediatrics. Originally published in "Zika Virus Infection in Pregnant Women in Rio de Janeiro – Preliminary Report" [21], reprinted with permission from NEJM

hydrocephalus once the fontanelles have closed, which occurs in up to 40% of children, often mandating VP shunt placement [20].

In contradistinction to Ebola virus, infection control does not pose limitations in the imaging of patients with Zika virus, as human-to-human transmission occurs only through sexual or vertical transmission. Diagnostic US, CT, or MRI can be performed while utilizing standard safety precautions and personal protective equipment. Radiology personnel must be aware of standard precautions, including the appropriate use of personal protective equipment, appropriate contact and airborne precautions, and the "5 moments for hand hygiene": before touching a patient; before any clean or aseptic procedure; after body fluid exposure risk; after touching a patient; and after touching a patient's surroundings [22]. Congenital Zika syndrome can have profound effects on cerebral development. Appropriate risk assessment along with early and frequent prenatal US evaluation can help detect fetal anomalies, including microcephaly and a spectrum of other intracranial manifestations. If available, more advanced imaging techniques such as CT or MRI can further characterize cerebral abnormalities and monitor for postnatal complications.

Chikungunya Fever

Chikungunya fever (CHIKF) is an infection caused by an RNA virus from the Togaviridae family transmitted to humans through the bite of infected Aedes aegypti and Aedes albopictus mosquitos [23], the same species responsible for the spread of Zika and Dengue viruses. The word "chikungunya" means to "walk bent over" in the Makonde language, spoken in southeast Tanzania and northern Mozambique, reflecting the severe arthralgia associated with the disease [24]. The virus was first isolated in 1955 following an outbreak on the Makonde Plateau in 1952. While periodic outbreaks have occurred over the last 50 years in Africa and Southeast Asia, large outbreaks in

Kenya in 2004 and in the west Indian Ocean region (Comoros, Mayotte, Mauritius, the Seychelles, and Reunion) in 2005 have led to a worldwide increased rate of disease, as well as travel-associated infection in non-endemic areas [23, 25, 26]. Cases in Brazil account for 94% of all confirmed cases in the Americas, and an additional large outbreak was described during the Olympic Games in Rio de Janeiro in 2016 [27].

Clinically, CHIKF can be divided into acute and chronic phases. The acute phase typically lasts 7 to 10 days and manifests with fever, rash, severe polyarthralgia involving the hands and feet, and fatigue (Fig. 2). Progression to the chronic phase, or "chronic migratory rheumatism," occurs in approximately 50% of patients over a span of 3 months to 3 years [23, 26, 27]. High expression of prostaglandins stimulates nociceptors that increase sensitivity to pain and increase osteoclastic activity, resulting in osseous erosion [28]. Additional sites of inflammation include lymph nodes, skin, liver, and spleen [29]. The chronic phase of disease is typically distal, symmetric, and polyarticular, involving the hands, wrists, and ankles [23]. Less common neurologic outcomes include seizure, encephalitis with decreased limb movements and extensor plantar response, and neuropathic pain [27]. The diagnosis is largely clinical with biochemical confirmation. Treatment is symptomatic, including anti-inflammatory medication. Antiviral treatment and vaccination are not currently available.

Musculoskeletal imaging (radiography, US, and MRI) is useful in assessing severity and extent of disease in the chronic phase. On hand radiographs, findings include periarticular osteopenia (18%), osteoarthritis (14%), soft tissue swelling (10%), and rarely marginal erosions (2%) [27]. Ultrasound shows tenosynovitis involving the small joints of the fingers, bulging of the joint capsule (84%), wrist effusions with incompressible synovial thickening (74%), finger flexor tenosynovitis (70%), cellulitis, wrist extensor tenosynovitis (38%), and thickening of the median nerve (36%) (Fig. 3) [23, 27]. MRI demonstrates similar findings, including tenosynovitis and polyarticular joint effusions, although erosive changes may be more apparent (Fig. 4) [24].

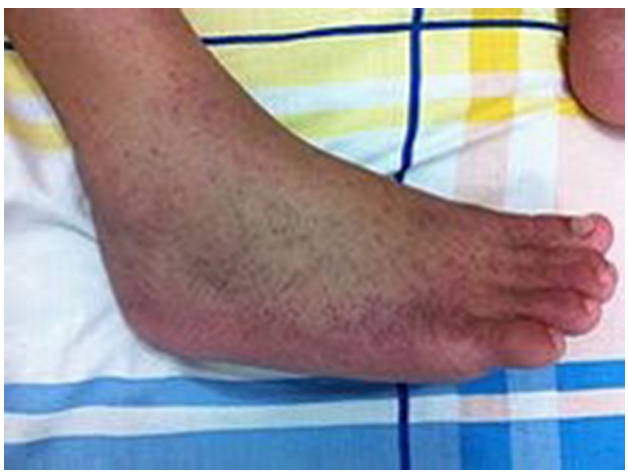

Fig. 2 Maculopapular rash of Chikungunya involving the right foot Image courtesy of Clarissa Canella, MD, Universidade Federal Fluminense, Rio De Janeiro, Brazil

Neuroimaging manifestations of CHIKF are non-specific and include restricted diffusion and fluid attenuation inversion recovery (FLAIR) signal abnormality in the bilateral frontoparietal white matter on MRI, with or without contrast enhancement. These imaging findings overlap with other viral encephalitides, demyelinating disease, vasculitides, and lymphoma. In the spine, characteristic enhancement and clumping of the nerve roots of the cauda equina has been described, although these findings can also be seen with West Nile Virus, arachnoiditis, and subarachnoid spread of tumor [25].

As there are no reports of human-to-human transmission of CHIKF, standard safety precautions and decontamination of surfaces and imaging equipment is sufficient for infection control in the healthcare setting.

While primarily a clinical diagnosis, the role of imaging in CHIKF is to assess the extent and severity of chronic musculoskeletal and rare extra-articular manifestations of disease and to monitor treatment response.

H1N1 Viral Influenza

H1N1 is an influenza A virus in the orthomyxovirus family that originated in Mexico in 2009. In the first influenza pandemic of the 21st century, the infection spread to more than 190 countries and territories, causing an estimated 61 million cases [30–32]. The H1N1 2009 influenza virus resulted from reassortment of multiple existing influenza strains including two swine strains, one avian strain, and one human strain, resulting in the name "swine flu" [33]. In contradistinction to seasonal influenza, the pandemic H1N1 infection was more virulent in younger adults, obese patients, and pregnant patients. In August 2010, the WHO announced that the H1N1 2009 influenza virus has moved into the post-pandemic period, and that the virus is expected to cause seasonal flu for years to come. During the 2013–2014 season, H1N1 was the predominant virus causing influenza-like illness, with significant morbidity and mortality [34]. Clinical features include fever, cough, rhinorrhea, dyspnea, myalgias, and gastrointestinal symptoms, with secondary complications ranging from bacterial pneumonia to acute respiratory distress syndrome (ARDS) [30]. Although the infection was mostly self-limited, 274,000 hospitalizations and 12,500 deaths were reported in 2009, and the CDC reported that 25% of hospitalized

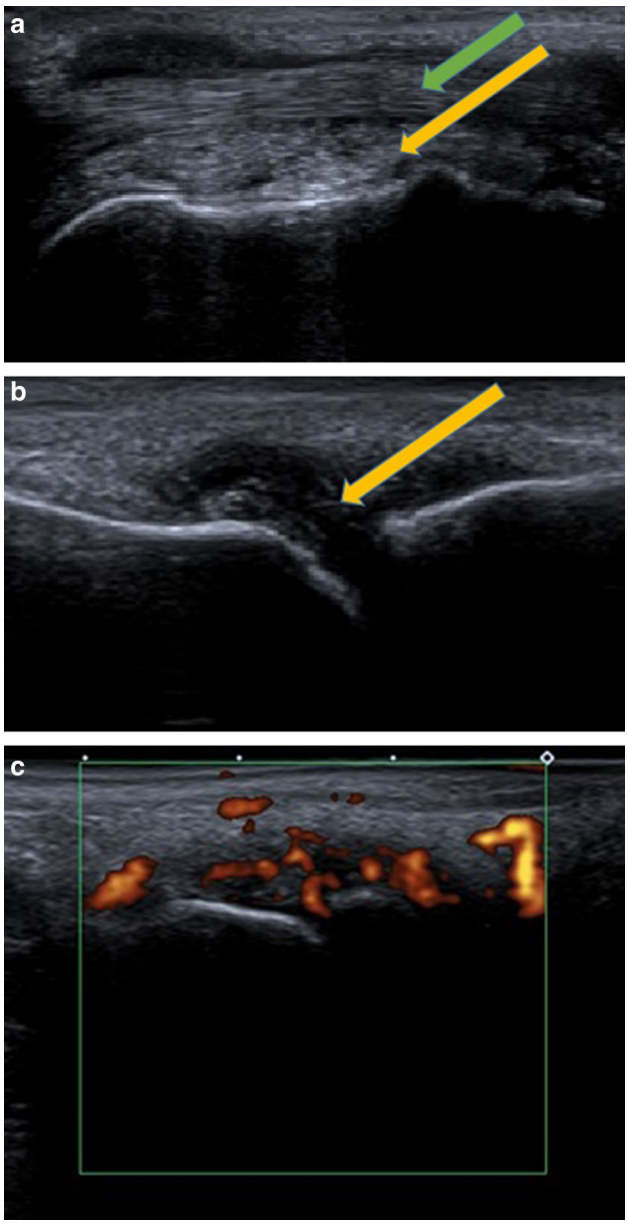

Fig. 3 A 22-year-old female with Chikungunya fever who presented with 6 weeks of polyarthritis and low-grade fever. **a** Longitudinal ultrasound of the posterior tibial tendon (green arrow) demonstrates fluid and synovial proliferation (yellow arrow), indicating tenosynovitis associated with late stage Chikungunya fever. **b** Longitudinal ultrasound of the 3rd metatarsophalangeal joint demonstrates similar synovial proliferation (yellow arrow). **c** Power Doppler images show increased flow, indicating synovitis of the 4th metatarsophalangeal joint Images courtesy of Clarissa Canella, MD, Universidade Federal Fluminense, Rio De Janeiro, Brazil (Color figure online)

patients required ICU admission [31, 32]. Treatment includes supportive measures, antivirals in patients at high risk of complications, and antibiotics for secondary bacterial infections.

Chest radiographs are the most frequently utilized study in the evaluation of H1N1 infection. Up to 56% of initial studies in H1N1-infected patients are normal [35, 36]. In severe cases or with disease progression, patients may rapidly develop bilateral ground glass opacities, consolidation, and reticular opacities, predominantly in the mid to lower lung zones [36–41]. Radiographic abnormalities correlate with disease progression, with bilateral, diffuse, peribronchovascular consolidation correlating with the subsequent need for mechanical ventilation and development of ARDS [41] (Fig. 5). Up to 67% of hospitalized patients with H1N1 will require mechanical ventilation [41]. Chest radiographs are also helpful in monitoring for short- and long-term complications of H1N1 infection, such as secondary bacterial pneumonia, ARDS, or pulmonary fibrosis (Figs. 6, 7).

While less accessible in resource-limited settings, CT is more sensitive in evaluation of H1N1 infection. The predominant CT features include multifocal peribronchovascular and/or subpleural ground glass opacities (Fig. 8) [35, 41]. Nodular opacities are seen in up to 60% of hospitalized patients [41]. These findings can progress to extensive bilateral consolidation and secondary bacterial pneumonia. Other sequela of acute infection include interlobular septal thickening and pulmonary edema due to ARDS, with more long-term complications including architectural distortion due to pulmonary fibrosis (Fig. 9) [35, 41].

Influenza is spread via infected bodily fluids. Therefore, standard droplet precautions are sufficient for imaging patients with H1N1 infection [30]. This includes wearing a mask when in close contact with infected individuals and decontaminating surfaces and imaging equipment with appropriate alcohol-based cleaning agents. Chest radiography can be safely and effectively implemented in resource-limited settings to diagnose and monitor H1N1 infection, including secondary complications which may require aggressive treatment.

Middle East Respiratory Syndrome (MERS)

MERS is a respiratory syndrome caused by a novel zoonotic coronavirus (Middle East respiratory syndrome coronavirus, MERS-CoV), initially isolated from a patient who died of severe respiratory illness in Saudi Arabia in 2012 [42]. Since 2012, major outbreaks have occurred in Saudi Arabia, United Arab Emirates, and the Republic of Korea, with 2279 laboratory-confirmed cases reported to the WHO from 27 countries [43]. The overall fatality rate is over 35%, with 806 deaths reported as of January 2019 [43]. Infected dromedary camels serve as the non-human reservoir for the virus, with the most common transmission being human-to-human through infected respiratory secretions, usually in the healthcare setting [43]. Clinically,

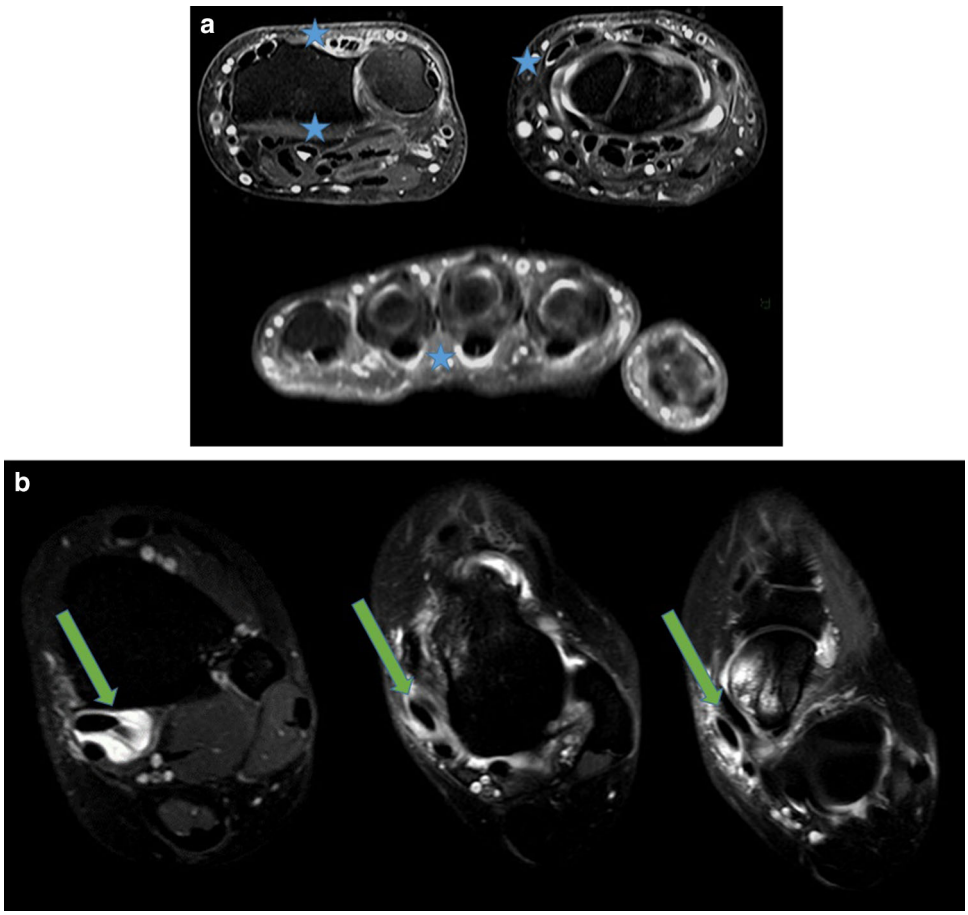

Fig. 4 Patient who presented for evaluation 4 months after onset of polyarthritis. **a** Axial T2 weighted MRI of the left wrist demonstrates synovitis of the radiocarpal and metacarpophalangeal joints, as well as tenosynovitis of multiple extensor and flexor tendons (blue stars). **b** Axial T2 weighted MRI of the left ankle in a patient with Chikungunya infection, 4 months after symptom onset, demonstrates tenosynovitis involving the posterior tibialis and flexor digitorum longus tendons (green arrows) Images courtesy of Clarissa Canella, MD, Universidade Federal Fluminense, Rio De Janeiro, Brazil

MERS can present as a broad spectrum of disease, from asymptomatic or mild disease to a rapidly progressive respiratory illness resulting in respiratory failure, septic shock, multi-organ failure, and death [44]. Children tend to present with less severe manifestations, with death only rarely reported if there are significant comorbidities [45–47].

More than 20% of MERS cases progress quickly to diffuse alveolar damage and ARDS [48]. Because of its fast and fulminant presentation, a high degree of clinical suspicion is needed in patients with recent potential exposure who present with an acute febrile illness, particularly if associated with lymphopenia and thrombocytopenia [49•]. Recent exposure includes a pertinent travel history to an endemic area or contact with a confirmed case of MERS within 2 weeks. A positive polymerase chain reaction laboratory test is required to confirm diagnosis [43, 49•]. Specific antiviral treatment and vaccination are not available.

Imaging plays a crucial role in early diagnosis, monitoring of disease progression, and prognostic evaluation. Radiologic features can be used to predict the severity of disease through a quantitative chest radiograph (CXR) or CT six-zone scoring system and identification of ancillary features that are negative prognostic indicators.

Initial CXR demonstrates abnormalities in 83% of cases [44]. The most common parenchymal abnormality is ground glass opacity (66% of patients), followed by consolidation (18%), or a combination of ground glass and consolidation (16%). Abnormalities are more frequently peripheral (58%) than central (25%) and most commonly involve the right lower lung (73%) (Fig. 10). On serial CXR and CT, patients typically show rapid progression of radiologic abnormalities [50].

Quantitative CXR scoring is performed by dividing each lung into three fields (upper, middle, and lower) and scoring each zone from 0 to 4, based on the percentage of the lung zone involved by abnormalities. A higher CXR score and the presence of pleural effusion or pneumothorax are associated with worse clinical outcome [44, 51]. Radiographic disease has also been classified into four patterns of progression based on the severe acute respiratory syndrome (SARS) system, which categorizes progression based on timing of peaks in radiographic abnormalities. Type 4 progression (progressive radiographic deterioration) is associated with a higher mortality

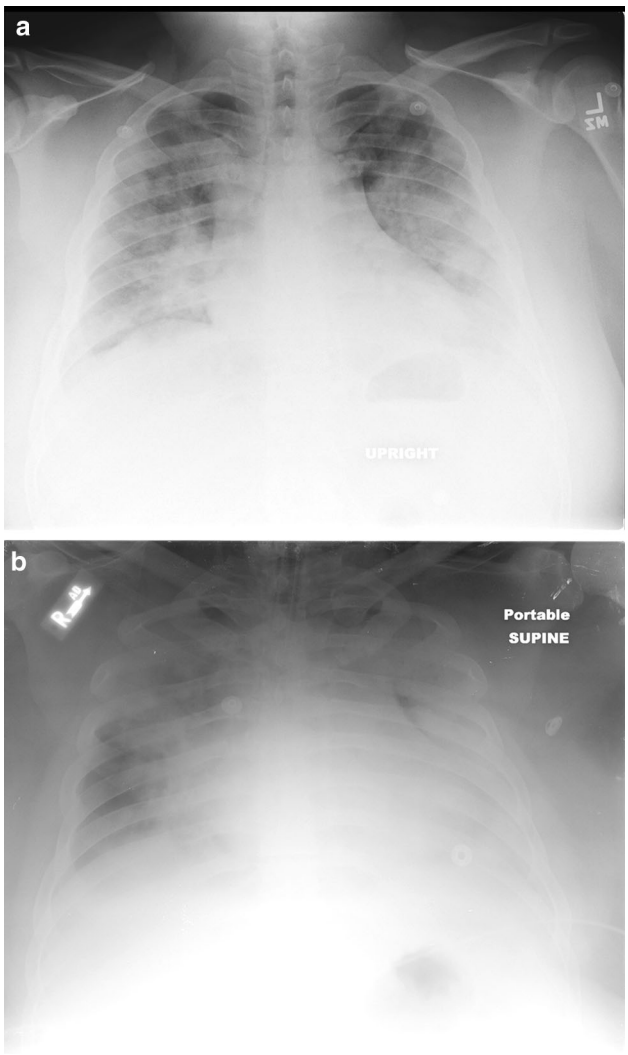

Fig. 5 A 34-year-old male with H1N1 influenza with rapid progression of disease. **a** Chest radiograph on the day of admission shows bilateral, symmetric ground glass and consolidation with (**b**) rapid progression of bilateral pulmonary opacities on hospital day 3. The patient ultimately required intubation and ICU admission

rate, which may be due to worsening of the primary MERS infection versus bacterial superinfection [44, 51, 52].

CT plays a more limited role in cases of confirmed MERS infection, although its higher sensitivity for subtle parenchymal abnormalities may be useful in patients with highly suspected disease but normal radiographs [49•]. The CT findings mirror CXR abnormalities, with ground glass opacity being most common (53% of cases), followed by ground glass opacity with consolidation (33%), consolidation (20%), and interlobular septal thickening (27%) [54]. More rarely and later in the disease course, crazy paving, tree-in-bud nodularity, organizing pneumonia, and cavitation have been described. While not typical of viral pneumonias, pleural effusions are noted in 33% of patients and serve as a poor prognostic indicator. As with CXR, CT

Fig. 6 A 45-year-old male with H1N1 influenza who required intubation. Focal consolidation in the right lower lobe on chest radiograph is consistent with superimposed bacterial pneumonia

Fig. 7 A 52-year-old male with H1N1 influenza with bilateral ground glass and consolidation and reticular opacities on chest radiograph

involvement can be quantified using the same six-zone scoring system, with a higher score associated with a higher mortality rate in adults [53]. While the incidence of abnormalities detected on CT appears lower than the corresponding CXR abnormalities, this is likely related to utilization of CT only in patients with high suspicion of disease whose CXRs were normal or showed only subtle abnormalities that required further characterization.

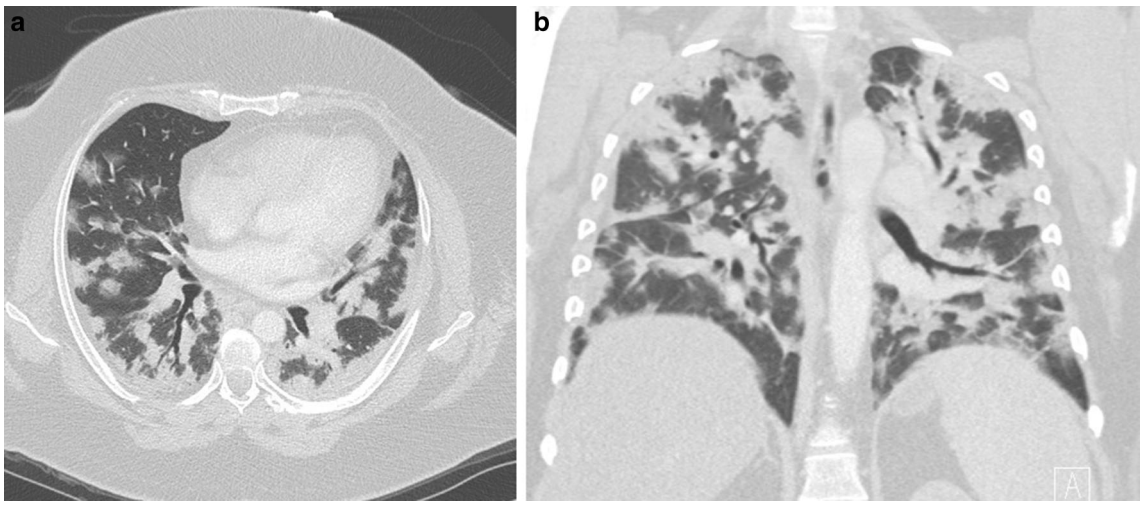

Fig. 8 A 42-year-old female who initially presented with fever and shortness of breath. **a** Axial and **b** coronal CT of the chest demonstrate diffuse peribronchovascular consolidation on CT, subsequently confirmed as H1N1 viral pneumonia

When there is confirmed or suspected MERS infection, appropriate patient isolation with airborne droplet precautions, as described for H1N1-infected individuals, are necessary to safely image the patients while preventing nosocomial transmission to healthcare workers and patients.

Severe Acute Respiratory Syndrome (SARS)

SARS is a respiratory illness caused by the zoonotic RNA human coronavirus group 2b (SARS-CoV) with some features similar to MERS [54]. While its definitive animal host is not clear, human transmission is thought to have originally occurred through the masked palm civet, with heavy human interaction in outdoor Chinese markets [54, 55]. An initial outbreak was reported in Guangdong Province in the People's Republic of China in 2002, with rapid spread to Hong Kong and subsequently 33 other countries over five continents. Healthcare workers were disproportionately affected, with most SARS exposures occurring in hospital settings. By the time the outbreak was contained in 2004, there were over 8000 confirmed cases and more than 800 reported deaths. Disease was more severe in the elderly, with a mortality rate of greater than 40% in patients over 60 years of age [55].

The clinical presentation of SARS includes flu-like symptoms with persistent fever and rapidly progressive dyspnea, with 20% of patients also presenting with watery diarrhea [55]. The WHO set criteria for "suspected" and "probable" SARS to aid in diagnosis. "Suspected" SARS was defined as high fever (> 38 °C), difficulty breathing/cough, and significant exposure to SARS. "Probable" SARS was defined as a suspected SARS with respiratory distress syndrome (RDS) or pneumonia on CXR, or suspected SARS with positive SARS-CoV laboratory assay [56]. As such, radiographic findings played a key role in appropriate triage and quarantine of potential SARS cases. Treatment is largely supportive, without specific antivirals or vaccines available.

Although 20% of patients initially present with a normal CXR, most cases develop significant abnormalities on subsequent imaging [57, 58]. When abnormal, initial CXR most commonly demonstrates a focal opacity, usually involving the peripheral mid to lower lung fields, with multifocal (27%) or diffuse (14%) opacities being less common [55, 57, 58]. CT has a higher sensitivity for small volume or subtle parenchymal disease and is likely to depict patchy consolidation and ground glass, even in early cases with normal CXR [57, 59]. Confluent opacities show rapid progression, often without associated mediastinal adenopathy, pleural effusion, or cavitation [60]. Consolidation peaks at approximately 6–9 days, usually coinciding with onset of steroid treatment, and resolves at a mean of 16 days [55, 56]. Chest radiographs that show more than one zone or bilateral parenchymal involvement, multifocal or diffuse opacities at baseline, or any pattern of progression other than initial deterioration to peak followed by improvement are associated with worse patient outcomes [58, 60]. Chronic chest CT findings typically develop 6–12 months after initial diagnosis and include intralobular and interlobular septal thickening, subpleural lines, and traction bronchiectasis [61]. Development of these chronic lung findings correlates with pulmonary function testing abnormalities [61].

Extrapulmonary radiographic manifestations of SARS are not widely reported in the literature, although SARS-CoV isolates have been found in the bowel, spleen, liver,

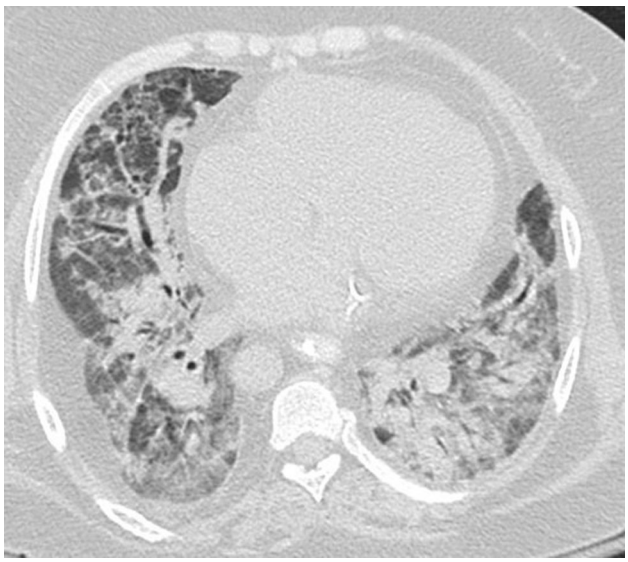

Fig. 9 A 30-year-old female with end-stage renal disease status post renal transplant who presented with H1N1 pneumonia that rapidly progressed to hypoxic respiratory failure and ARDS

Fig. 10 A 40-year-old female with multiple medical comorbidities who initially presented with fever and severe cough, subsequently confirmed as MERS. Chest radiograph on admission to the ICU showed extensive air space consolidation in the right mid and the lower lung zones with ground glass opacities in the left mid lung zone. This patient expired 5 days after admission Image courtesy of Dr. K.M. Das, MD, FSCCT, Department of Radiology, College of Medicine and Health Science, UAE University, United Arab Emirates

lymph nodes, and kidneys at autopsy [57]. Because many SARS patients received high-dose corticosteroids, osteonecrosis and decreased bone density have been reported [62, 63].

Similar to patients with suspected MERS infection, appropriate isolation of the SARS-infected patient is important to prevent nosocomial transmission. Patients should be screened and appropriately isolated and masked for safe imaging and diagnosis. In the 2003 outbreak, 75% of SARS cases in Singapore were contracted in the hospital setting, with 10 cases directly linked to the imaging department [64•]. This highlights the importance of early suspicion and appropriate isolation, specifically within the imaging department.

Conclusion

Imaging plays a variable but important role in the management of emerging infectious diseases. Emerging infectious diseases often arise in resource-limited settings, where radiography and ultrasound can contribute to initial diagnosis and monitoring of disease complications. CT and MRI, when available, also contribute to evaluation of disease progression. In the setting of highly contagious disease entities such as SARS or Ebola, it is imperative to understand methods of disease transmission, as well as adhere to appropriate disinfection protocols while imaging to limit nosocomial disease spread. As new disease outbreaks are unpredictable and can spread rapidly, it is important for radiologists to recognize the impact medical imaging can have on the global dissemination of these highly infectious disease agents.

Acknowledgements We would like to express our great appreciation to the following individuals who provided their expertise as well as sample imaging for entities not routinely encountered in our own clinical practices: Drs. Karin Nielsen and Kristina Adachi from the Department of Pediatrics at UCLA (ZVD); Dr. Clarissa Canella from the Department of Radiology at Universidade Federal Fluminense, Rio De Janeiro (CHIKF); and Dr. KM Das from the Department of Radiology at the College of Medicine & Health Sciences at UAE University (MERS).

Compliance with Ethical Standards

Conflict of interest All the authors declared that they have no potential conflicts of interest.

References

Recently published papers of particular interest have been highlighted as:

- • Of importance
- •• Of major importance

1. World Health Organization. The World Health Report 2007: a safer future: global public health security in the 21st century, 2007, ISBN 978 92 4 156344 4. https://www.who.int/whr/2007/en/. Accessed 1 Feb 2019.
2. The National Institute for Occupational Safety and Health. Emerging Infectious Diseases, 2018, Centers for Disease Control,

https://www.cdc.gov/niosh/topics/emerginfectdiseases/default.html. Accessed 1 Feb 2019.
3. Holmes EC, Dudas G, Rambaut A, Andersen KG. The evolution of Ebola virus: insights from the 2013-2016 epidemic. Nature. 2016;538(7624):193–200. https://doi.org/10.1038/nature19790.
4. World Health Organization. Ebola Virus Disease, 2018. https://www.who.int/news-room/fact-sheets/detail/ebola-virus-disease. Accessed 1 Feb 2019.
5. Centers for Disease Control. Ebola in Democratic Republic of the Congo, 2018. http://wwwnc.cdc.gov/trave/notices/alert/ebola-democratic-republic-of-the-congo. Accessed 1 Feb 2019.
6. Vetter P, Fischer WA II, Schibler M, Jacobs M, Bausch DG, Kaiser L. Ebola virus shedding and transmission: review of current evidence. J Infect Dis. 2016;214(suppl 3):S177–84. https://doi.org/10.1093/infdis/jiw254.
7. Vogl TJ, Martin S, Brodt HR, Keppler O, Zacharowski K, Wolf T. The Frankfurt Ebola patient. RoFo: Fortschritte auf dem Gebiete der Rontgenstrahlen und der Nuklearmedizin. 2015;187(9):771–6. https://doi.org/10.1055/s-0035-1553130.
8. •• Moreno CC, Kraft CS, Vanairsdale S, Kandiah P, Klopman MA, Ribner BS et al. Performance of bedside diagnostic ultrasound in an Ebola isolation unit: the Emory University Hospital experience. AJR Am J Roentgenol. 2015;204(6):1157–9. https://doi.org/10.2214/ajr.15.14344. *This paper details Emory University's initial successful treatment of Ebola patients in their specialized isolation unit, where portable ultrasound techniques were safely utilized without nosocomial spread of infection.*
9. Busi Rizzi E, Puro V, Schinina V, Nicastri E, Petrosillo N, Ippolito G. Radiographic imaging in Ebola virus disease: protocol to acquire chest radiographs. Eur Radiol. 2015;25(11):3368–71. https://doi.org/10.1007/s00330-015-3748-6.
10. Johnston AM, Lewis SE. Decontaminating Ebola-infected ultrasound probes. Anaesthesia. 2015;70(5):628–9. https://doi.org/10.1111/anae.13060.
11. Mollura DJ, Palmore TN, Folio LR, Bluemke DA. Radiology preparedness in ebola virus disease: guidelines and challenges for disinfection of medical imaging equipment for the protection of staff and patients. Radiology. 2015;275(2):538–44. https://doi.org/10.1148/radiol.15142670.
12. Auffermann WF, Kraft CS, Vanairsdale S, Lyon GM 3rd, Tridandapani S. Radiographic imaging for patients with contagious infectious diseases: how to acquire chest radiographs of patients infected with the Ebola virus. AJR Am J Roentgenol. 2015;204(1):44–8. https://doi.org/10.2214/ajr.14.14041.
13. Abi-Jaoudeh N, Walser EM, Bartal G, Cohen AM, Collins JD, Gross KA, et al. Ebola and other highly contagious diseases: strategies by the society of interventional radiology for interventional radiology. J Vasc Interven Radiol. 2016;27(2):200–2. https://doi.org/10.1016/j.jvir.2015.10.014.
14. Musso D, Gubler DJ. Zika virus. Clin Microbiol Rev. 2016;29(3):487–524. https://doi.org/10.1128/cmr.00072-15.
15. Parra-Saavedra M, Reefhuis J, Piraquive JP, Gilboa SM, Badell ML, Moore CA, et al. Serial head and brain imaging of 17 fetuses with confirmed zika virus infection in Colombia, South America. Obstet Gynecol. 2017;130(1):207–12. https://doi.org/10.1097/aog.0000000000002105.
16. da Hygino Cruz LC Jr, Nascimento OJM, Lopes F, da Silva IRF. Neuroimaging findings of zika virus-associated neurologic complications in adults. AJNR Am J Neuroradiol. 2018;39(11):1967–74. https://doi.org/10.3174/ajnr.A5649.
17. World Health Organization. Zika Strategic Response Plan, 2016. https://www.who.int/emergencies/zika-virus/strategic-response-plan/en/. Accessed 1 Feb 2019.
18. • Zare Mehrjardi M, Poretti A, Huisman TA, Werner H, Keshavarz E, Araujo Junior E. Neuroimaging findings of congenital Zika virus infection: a pictorial essay. Jpn J Radiol. 2017;35(3):89–94. https://doi.org/10.1007/s11604-016-0609-4. *This paper provides a detailed multi-modality overview of imaging findings associated with congenital Zika infection.*
19. Levine D, Jani JC, Castro-Aragon I, Cannie M. How does imaging of congenital zika compare with imaging of other TORCH infections? Radiology. 2017;285(3):744–61. https://doi.org/10.1148/radiol.2017171238.
20. Petribu NCL, Aragao MFV, van der Linden V, Parizel P, Jungmann P, Araujo L, et al. Follow-up brain imaging of 37 children with congenital Zika syndrome: case series study. BMJ. 2017;359:j4188. https://doi.org/10.1136/bmj.j4188.
21. Brasil P, Pereira JP Jr, Moreira ME, Ribeiro Nogueira RM, Damasceno L, Wakimoto M, et al. Zika virus infection in pregnant women in Rio de Janeiro. N Engl J Med. 2016;375(24):2321–34. https://doi.org/10.1056/NEJMoa1602412.
22. World Health Organization. Infection prevention and control during health care for probable or confirmed cases of Middle East respiratory syndrome coronavirus (MERS-CoV) infection, 2015. https://apps.who.int/iris/handle/10665/174652. Accessed 1 Feb 2019.
23. Canella C. Imaging findings in chikungunya fever. Radiologia brasileira. 2017;V(2):V. https://doi.org/10.1590/0100-3984.2017.50.2e1.
24. Mizuno Y, Kato Y, Takeshita N, Ujiie M, Kobayashi T, Kanagawa S, et al. Clinical and radiological features of imported chikungunya fever in Japan: a study of six cases at the National Center for Global Health and Medicine. J Infect Chemother. 2011;17(3):419–23. https://doi.org/10.1007/s10156-010-0124-y.
25. Ganesan K, Diwan A, Shankar SK, Desai SB, Sainani GS, Katrak SM. Chikungunya encephalomyeloradiculitis: report of 2 cases with neuroimaging and 1 case with autopsy findings. AJNR Am J Neuroradiol. 2008;29(9):1636–7. https://doi.org/10.3174/ajnr.A1133.
26. Alfaro-Toloza P, Clouet-Huerta DE, Rodriguez-Morales AJ. Chikungunya, the emerging migratory rheumatism. Lancet Infect Dis. 2015;15(5):510–2. https://doi.org/10.1016/s1473-3099(15)70160-x.
27. Mogami R, Vaz JLP, de Chagas YFB, de Abreu MM, Torezani RS, de Almeida Vieira A, et al. Ultrasonography of hands and wrists in the diagnosis of complications of chikungunya fever. J Ultrasound Med. 2018;37(2):511–20. https://doi.org/10.1002/jum.14344.
28. Chen W, Foo SS, Sims NA, Herrero LJ, Walsh NC, Mahalingam S. Arthritogenic alphaviruses: new insights into arthritis and bone pathology. Trends Microbiol. 2015;23(1):35–43. https://doi.org/10.1016/j.tim.2014.09.005.
29. Rose MV, Kjaer ASL, Markova E, Graff J. (18)F-FDG PET/CT findings in a patient with chikungunya virus infection. Diagnostics (Basel, Switzerland). 2017. https://doi.org/10.3390/diagnostics7030049.
30. Rewar S, Mirdha D, Rewar P. Treatment and prevention of pandemic H1N1 influenza. Ann Glob Health. 2015;81(5):645–53. https://doi.org/10.1016/j.aogh.2015.08.014.
31. Bramley AM, Dasgupta S, Skarbinski J, Kamimoto L, Fry AM, Finelli L, et al. Intensive care unit patients with 2009 pandemic influenza A (H1N1pdm09) virus infection - United States, 2009. Influenza Other Respir Vir. 2012;6(6):e134–42. https://doi.org/10.1111/j.1750-2659.2012.00385.x.
32. Webb SA, Pettila V, Seppelt I, Bellomo R, Bailey M, Cooper DJ, et al. Critical care services and 2009 H1N1 influenza in Australia and New Zealand. N Engl J Med. 2009;361(20):1925–34. https://doi.org/10.1056/NEJMoa0908481.
33. Patel M, Dennis A, Flutter C, Khan Z. Pandemic (H1N1) 2009 influenza. Br J Anaesth. 2010;104(2):128–42. https://doi.org/10.1093/bja/aep375.
34. Centers for Disease Control. Situation Update: Summary of Weekly FluView,2014. http://www.cdc.gov/flu/weekly/summary.htm. Accessed 1 Feb 2014.

35. Li P, Zhang JF, Xia XD, Su DJ, Liu BL, Zhao DL, et al. Serial evaluation of high-resolution CT findings in patients with pneumonia in novel swine-origin influenza A (H1N1) virus infection. Br J Radiol. 2012;85(1014):729–35. https://doi.org/10.1259/bjr/85580974.
36. Norzailin AB, Norhafizah E. Chest radiograph findings in novel swine-origin influenza A (H1N1) virus (S-OIV) infection: a UKMMC experience. Med J Malays. 2015;70(2):93–7.
37. Pirakalathanan J, Lau KK, Joosten SA. Chest radiographic appearances in adult inpatients admitted with swine flu infection: local experience in Melbourne. J Med Imaging Radiat Oncol. 2013;57(1):50–6. https://doi.org/10.1111/j.1754-9485.2012.02415.x.
38. Bakhshayeshkaram M, Saidi B, Tabarsi P, Zahirifard S, Ghofrani M. Imaging findings in patients with H1N1 influenza A infection. Iran J Radiol. 2011;8(4):230–4. https://doi.org/10.5812/iranjradiol.4554.
39. Jartti A, Rauvala E, Kauma H, Renko M, Kunnari M, Syrjala H. Chest imaging findings in hospitalized patients with H1N1 influenza. Acta Radiologica (Stockholm, Sweden: 1987). 2011;52(3):297–304. https://doi.org/10.1258/ar.2010.100379.
40. Louie JK, Acosta M, Winter K, Jean C, Gavali S, Schechter R, et al. Factors associated with death or hospitalization due to pandemic 2009 influenza A(H1N1) infection in California. JAMA. 2009;302(17):1896–902. https://doi.org/10.1001/jama.2009.1583.
41. Rohani P, Jude CM, Chan K, Barot N, Kamangar N. Chest radiological findings of patients with severe H1N1 pneumonia requiring intensive care. J Intensive Care Med. 2016;31(1):51–60. https://doi.org/10.1177/0885066614538753.
42. Assiri A, Al-Tawfiq JA, Al-Rabeeah AA, Al-Rabiah FA, Al-Hajjar S, Al-Barrak A, et al. Epidemiological, demographic, and clinical characteristics of 47 cases of Middle East respiratory syndrome coronavirus disease from Saudi Arabia: a descriptive study. Lancet Infect Dis. 2013;13(9):752–61. https://doi.org/10.1016/s1473-3099(13)70204-4.
43. World Health Organization. WHO MERS Global Summary and Assessment of Risk, 2018. https://www.who.int/emergencies/mers-cov/en/. Accessed 1 Feb 2019.
44. Das KM, Lee EY, Al Jawder SE, Enani MA, Singh R, Skakni L, et al. Acute Middle East respiratory syndrome coronavirus: temporal lung changes observed on the chest radiographs of 55 patients. AJR Am J Roentgenol. 2015;205(3):W267–74. https://doi.org/10.2214/ajr.15.14445.
45. Memish ZA, Al-Tawfiq JA, Assiri A, AlRabiah FA, Al Hajjar S, Albarrak A, et al. Middle East respiratory syndrome coronavirus disease in children. Pediatr Infect Dis J. 2014;33(9):904–6. https://doi.org/10.1097/inf.0000000000000325.
46. Al-Tawfiq JA, Kattan RF, Memish ZA. Middle East respiratory syndrome coronavirus disease is rare in children: an update from Saudi Arabia. World J Clin Pediatr. 2016;5(4):391–6. https://doi.org/10.5409/wjcp.v5.i4.391.
47. Das KM, Lee EY. Middle East respiratory syndrome coronavirus in children. Indian Pediatr. 2016;53(8):752.
48. Assiri A, McGeer A, Perl TM, Price CS, Al Rabeeah AA, Cummings DA, et al. Hospital outbreak of Middle East respiratory syndrome coronavirus. N Engl J Med. 2013;369(5):407–16. https://doi.org/10.1056/NEJMoa1306742.
49. • Das KM, Lee EY, Langer RD, Larsson SG. Middle East respiratory syndrome coronavirus: what does a radiologist need to know? Am J Roentgenol. 2016;206:1193–201. https://doi.org/10.2214/ajr.15.15363. *This paper provides a detailed overview of clinical and imaging findings of MERS-CoV, as well as a detailed scoring system which allows for prediction of patient outcomes based on chest radiography findings.*
50. Choi WJ, Lee KN, Kang EJ, Lee H. Middle East respiratory syndrome-coronavirus infection: a case report of serial computed tomographic findings in a young male patient. Korean J Radiol. 2016;17(1):166–70. https://doi.org/10.3348/kjr.2016.17.1.166.
51. Cha MJ, Chung MJ, Kim K, Lee KS, Kim TJ, Kim TS. Clinical implication of radiographic scores in acute Middle East respiratory syndrome coronavirus pneumonia: report from a single tertiary-referral center of South Korea. Eur J Radiol. 2018;107:196–202. https://doi.org/10.1016/j.ejrad.2018.09.008.
52. Wong KT, Antonio GE, Hui DS, Lee N, Yuen EH, Wu A, et al. Severe acute respiratory syndrome: radiographic appearances and pattern of progression in 138 patients. Radiology. 2003;228(2):401–6. https://doi.org/10.1148/radiol.2282030593.
53. Das KM, Lee EY, Enani MA, AlJawder SE, Singh R, Bashir S, et al. CT correlation with outcomes in 15 patients with acute Middle East respiratory syndrome coronavirus. AJR Am J Roentgenol. 2015;204(4):736–42. https://doi.org/10.2214/ajr.14.13671.
54. Hui DS, Memish ZA, Zumla A. Severe acute respiratory syndrome vs. the Middle East respiratory syndrome. Curr Opin Pulm Med. 2014;20(3):233–41. https://doi.org/10.1097/mcp.0000000000000046.
55. Cleri DJ, Ricketti AJ, Vernaleo JR. Severe acute respiratory syndrome (SARS). Infect Dis Clin N Am. 2010;24(1):175–202. https://doi.org/10.1016/j.idc.2009.10.005.
56. Case Definitions for Surveillance of Severe Acute Respiratory Syndrome (SARS). 2003.
57. Paul NS, Roberts H, Butany J, Chung T, Gold W, Mehta S, et al. Radiologic pattern of disease in patients with severe acute respiratory syndrome: the Toronto experience. Radiographics. 2004;24(2):553–63. https://doi.org/10.1148/rg.242035193.
58. Hui DS, Wong KT, Antonio GE, Ahuja A, Sung JJ. Correlation of clinical outcomes and radiographic features in SARS patients. Hong Kong Med J. 2009;15(Suppl 8):24–8.
59. Kirsch J, Ramirez J, Mohammed TL, Amorosa JK, Brown K, Dyer DS, et al. ACR Appropriateness Criteria(R) acute respiratory illness in immunocompetent patients. J Thorac Imaging. 2011;26(2):W42–4. https://doi.org/10.1097/RTI.0b013e31820ffe0f.
60. Wan YL, Tsay PK, Cheung YC, Chiang PC, Wang CH, Tsai YH, et al. A correlation between the severity of lung lesions on radiographs and clinical findings in patients with severe acute respiratory syndrome. Korean J Radiol. 2007;8(6):466–74. https://doi.org/10.3348/kjr.2007.8.6.466.
61. Wu X, Dong D, Ma D. Thin-section computed tomography manifestations during convalescence and long-term follow-up of patients with severe acute respiratory syndrome (SARS). Med Sci Monit. 2016;22:2793–9.
62. Griffith JF. Musculoskeletal complications of severe acute respiratory syndrome. Semin Musculoskelet Radiol. 2011;15(5):554–60. https://doi.org/10.1055/s-0031-1293500.
63. Li YM, Wang SX, Gao HS, Wang JG, Wei CS, Chen LM, et al. Factors of avascular necrosis of femoral head and osteoporosis in SARS patients' convalescence. Zhonghua yi xue za zhi. 2004;84(16):1348–53.
64. • Gogna A, Tay KH, Tan BS. Severe acute respiratory syndrome: 11 years later–a radiology perspective. AJR Am J Roentgenol. 2014;203(4):746–8. https://doi.org/10.2214/ajr.14.13062. *This paper reflects on the SARS pandemic of 2003 and highlights the importance of safe imaging practices in limiting the spread of highly infectious diseases.*